

Self-Assembly Effect during the Adsorption of Polynucleotides on Stearic Acid Langmuir–Blodgett Monolayer

Evgeniy V. Dubrovin,^{*,†} Sergey N. Staritsyn,[‡] Sergey A. Yakovenko,[‡] and Igor V. Yaminsky[†]

Department of Physics of Polymers and Crystals and Department of Biophysics, Faculty of Physics, Moscow State University, Leninskie Gory, 1/2, Moscow 119992, Russia

Received February 21, 2007; Revised Manuscript Received May 15, 2007

Interaction of polyadenylic acid, poly(A), with stearic acid Langmuir–Blodgett (LB) monolayer was studied in different electrolyte surroundings. For this purpose LB films of stearic acid, transferred on the mica substrate from poly(A) containing subphase, were analyzed with atomic force microscopy (AFM). The density of polynucleotides surface coverage is ruled by the monovalent electrolyte concentration in the subphase that is in good agreement with previous results. Divalent cations in the subphase are needed to stabilize poly(A) molecules on the surface through formation of “salt bridges”. At the very low divalent electrolyte concentration polynucleotides adsorb on the LB film to domains in which the effect of self-assembly is observed. Increase of divalent electrolyte concentration leads to the loss of this orientation effect. The explanation of this effect is proposed.

Introduction

Investigation of polynucleotide assemblies is currently of strong interest in biotechnology. Due to their unique recognition capabilities, physicochemical stability, mechanical rigidity, and possibilities for repeated denaturation–hybridization cycles, polynucleotides and their complexes are increasingly used in technological and medical applications, e.g., as DNA microarrays for genomics,¹ as biosensors,^{2,3} and nanowires,⁴ etc.

Another possible application is the use of DNA–cationic lipid complexes for gene delivery.⁵ A variety of such complexes has been investigated, including DNA adsorption to cationic lipid bilayers,⁶ DNA complexes with Langmuir monolayers of cationic lipid octadecylamine,⁷ DNA–cationic liposome complexes,⁸ and creation of multilayered films of nucleic acids and polycations.⁹ The build-up mechanism of most polynucleotide complexes consists mainly of electrostatic interaction between the oppositely charged molecules.¹⁰

Budker et al.^{11,12} have shown the important role of divalent ions in the interactions between polynucleotides and zwitterionic lipid (phosphatidylcholine) membranes. These experiments provide strong evidence that there is no direct electrostatic interaction between zwitterionic lipids and DNA, but the interaction is mediated by divalent cations by formation of salt (Mg^{2+}) bridges between phosphate residues of polynucleotides and phosphate groups in phospholipids. Nevertheless, the mechanisms leading to the formation of polynucleotides and zwitterionic lipid complexes are still under consideration.¹³

However, there is a lack of investigation of nucleic acid–anionic lipid complexes, although Patil et al.¹⁴ have shown that transfection efficiency of anionic liposomes is similar to that of cationic ones, whereas their toxicity is significantly lower. It is possible to prepare aggregates from like-charged surfactants and polymers by mediating the electrostatic attraction using multivalent counterions. For example, the immobilization of long

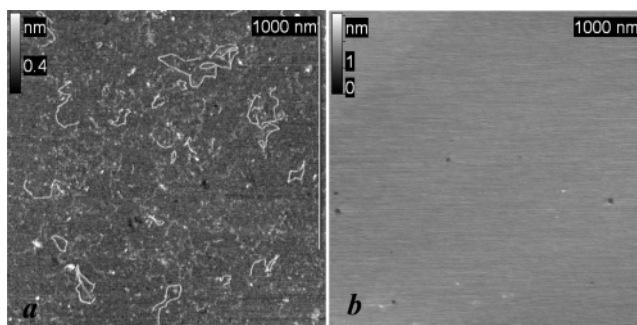


Figure 1. AFM images of (a) poly(A) molecules immobilized on the APTES-treated mica and (b) stearic acid Langmuir monolayer transferred on the freshly cleaved mica surface. Scan sizes are 1.37 (a) and 3.47 μm (b).

dsDNA on a fatty acids monolayer was demonstrated with the help of Zn coordination and biological activity of immobilized DNA.¹⁵

We are interested in fabrication of polynucleotide complexes with anionic molecules. In this work we aimed to investigate the behavior of polyadenylic acid (poly(A)) molecules at the surface of stearic acid monolayer and to study their interaction in different electrolyte surroundings. We used here Langmuir–Blodgett (LB) technique as the tool of creation of the monolayer and its transfer onto the substrate and atomic force microscopy (AFM) for analysis of obtained structures. These techniques have already approved themselves for investigation of different DNA/RNA complexes.^{7–9}

Materials and Methods

Polyadenylic, stearic acids, and ethylenediaminetetraacetic (EDTA) were purchased from Sigma. The sodium chloride was USP-grade (>99.99%, Akzo Nobel). All reagents were used without additional purification. The polynucleotides have molecular mass of 10^5 – 10^6 Da (Sigma data), which corresponds to 300–3000 nucleotides in single-strand chain. The polynucleotide concentration in the subphase was 0.001 mg/mL (molar concentration $\sim 3 \times 10^{-6}$ M of monomer units).

* To whom correspondence should be addressed. E-mail: dubrovin@genebee.msu.ru.

[†] Department of Physics of Polymers and Crystals.

[‡] Department of Biophysics.

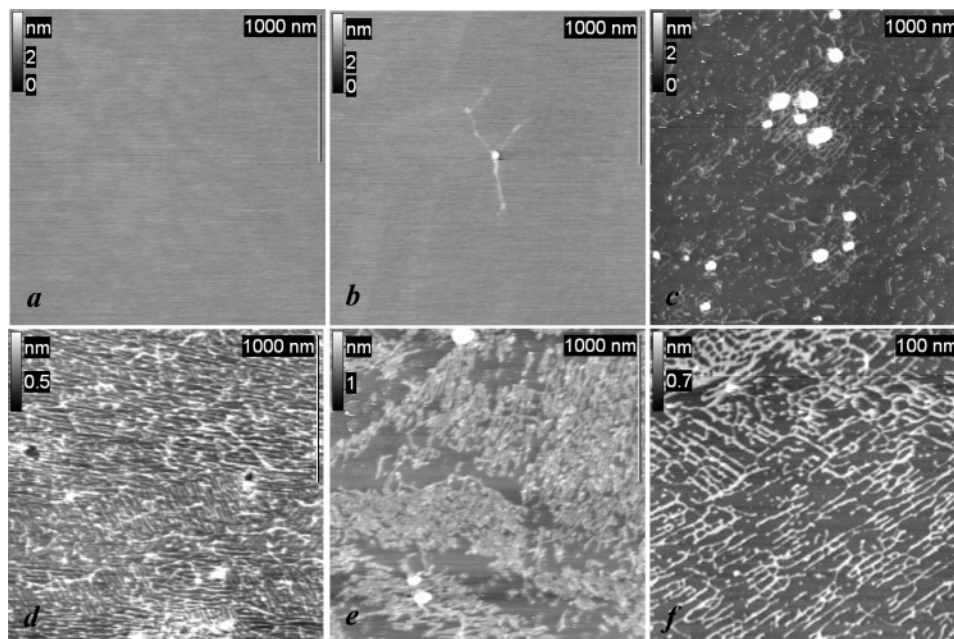


Figure 2. AFM images of stearic acid LB monolayers transferred from the subphase containing polyA (10^{-3} mg/mL). The NaCl concentration in the subphase was (a) 0 M, (b) 10 mM, (c) 100 mM, (d) 500 mM, and (e, f) 1 M. Image sizes (a–e) 2.14 and (f) 1.09 μm .

Monolayers were prepared in a Langmuir trough with dimensions $14 \times 25 \text{ cm}^2$. The deionized water (Millipore Milli-Q system) with resistivity no less than $18 \text{ M}\Omega\cdot\text{cm}$ was used in all experiments. The temperature was 20°C .

Stearic acid was dissolved in chloroform (spectroscopic grade) to obtain 1 mM solution. The absence of a pressure–area isotherm after evaporation of chloroform from the water–air interface indicated that neither chloroform nor its possible contaminants contribute to the isotherms. After surfactant deposition onto the subphase, the monolayer was stored during 10 min before its compression (30 min if the subphase contained a polynucleotide). In the case of a polynucleotide free subphase, the shape of the pressure–area curves for the surfactants did not depend on the time period of the monolayer storage (10 or 30 min) before compression.

For the atomic force microscopy (AFM) studies the monolayer was transferred by vertical dipping method onto a mica surface: at first a freshly cleaved mica plate with a vertically oriented surface was immersed into the bath, and then it was withdrawn with the speed of 3 mm/min. The monolayer was transferred only during withdrawal of the substrate. The substrate was passed through the monolayer one time. The surface pressure (18 mN/m) was kept constant during the monolayer transfer procedure.

All the AFM measurements were recorded in air using a Nanoscope IIIa microscope (Digital Instruments, Santa Barbara, CA) equipped with $15 \mu\text{m}$ scanner in the tapping mode of scanning. The commercial silicon cantilevers had 42 N/m stiffness; their resonance frequency was in the range of 280–310 kHz. The scan frequency was about 2 Hz. Image processing was performed using FemtoScan software.¹⁶

Results and Discussion

Figure 1a represents a typical AFM image of poly(A) molecules used in our experiments. This image was obtained on the specimen that was prepared using conventional technique of DNA immobilization on an APTES-modified mica surface.¹⁷ The height and the width of the molecules measured on the half-height are 0.7–0.8 and 8–10 nm correspondingly, which is consistent with previous results, where AFM images of poly(A) molecules were obtained in tapping mode.¹⁸ The measured heights and widths cannot, however, be considered as true dimensions of poly(A) molecules due to the well-known

broadening effect of the AFM tip and its slight compression effect.¹⁹ It should be noted that the broadening effect depends strongly on the tip radius (which we did not control), and therefore we use the width value only for rough estimations. The measured contour lengths of poly(A) molecules on the substrate vary from several tens of nanometers to 500 nm, which is in a good agreement with the molecular mass distribution of the polyadenylic acid used (see Materials and Methods).

AFM images of stearic acid LB monolayer, transferred onto the mica substrate from the subphase free from nucleic acids, either containing ions or not, represent a smooth homogeneous surface with rare defects (holes) (Figure 1b). The number of holes in the monolayer and their depth (the hole can be also made artificially by AFM tip if needed) help to control the quality of the obtained monolayer. In our experiments we have created monolayers with less than 1% of defects on the surface (in the meaning). Additional evidence of the successful monolayer transfer is the change of hydrophobic properties of the surface after its dipping in the trough, which was detected by considerable change of the contact angle (data not shown). Stearic acid monolayer modified mica becomes hydrophobic due to exposed hydrocarbon tails of fatty acid.

AFM images of the specimens obtained from the subphase containing poly(A) and 1 mM of NaCl (or without any salt at all) look similar to control images of stearic acid monolayer (Figure 2a). Double-layer electrostatic repulsion of two like-charged negative surfaces prevents the adsorption of poly(A) on the monolayer to take place. In the presence of 10 mM NaCl in the subphase some solitary fibers can be observed in the corresponding AFM images (Figure 2b). The lengths of these fibers coincide with lengths of poly(A) molecules in the control images (Figure 1a), and therefore we assume that here we also observe poly(A) molecules. The increase in concentration of sodium chloride in the subphase results in the increase of the surface density of poly(A) fibers visualized on the monolayer (Figure 2c–f). Topographical features observed in Figure 3c as white spots could be aggregated poly(A). When sodium chloride concentration in the subphase constitutes 500 mM, it becomes clearly seen that poly(A) molecules form the domains of stretched parallel molecules on the monolayer and each

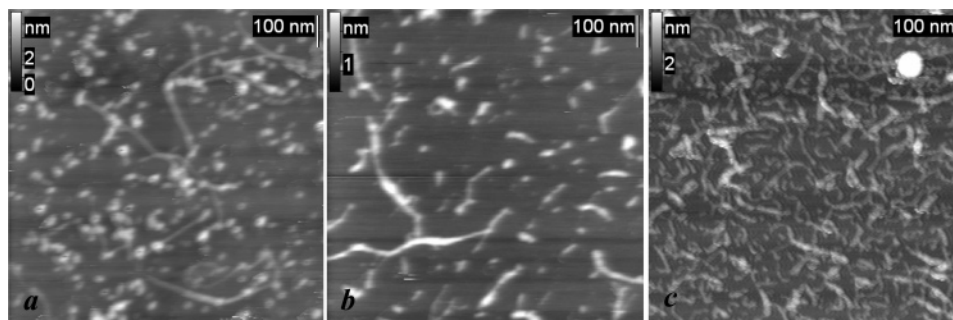


Figure 3. AFM images of stearic acid LB monolayers transferred from the subphase containing poly(A) (10^{-3} mg/mL) and MgCl_2 (1 mM). NaCl concentration in the subphase was (a) 0 M, (b) 100 mM, and (c) 500 mM. Image sizes are $1 \times 1 \mu\text{m}^2$.

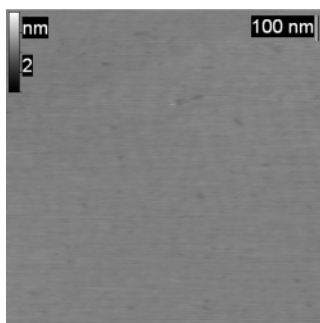


Figure 4. AFM image of stearic acid LB monolayer transferred from the subphase containing poly(A) (10^{-3} mg/mL), NaCl (1 M), and EDTA (10 mM). The scan size is $1.27 \times 1.27 \mu\text{m}^2$.

domain has its own direction of alignment. These structures are well-reproduced and uniform throughout the full surface of the sample. AFM images were stable, and observed structures were not somehow damaged or modified by the AFM tip during measurements. There is no detectable correlation between the directions of poly(A) domains on the mica surface and the direction of its withdrawal during monolayer transfer. This testifies that the orientation effect took place prior to the monolayer transfer. Stearic acid LB monolayer is transferred by COOH groups to the mica surface and hydrocarbon chains exhibited out of surface. This means that on our samples poly(A) molecules are sandwiched between mica and stearic acid monolayer.

Addition of divalent ions (Mg^{2+} , 1 mM) into the subphase induces the intense complexation of poly(A) with stearic acid monolayer. The amount of adsorbed poly(A) molecules is practically constant in the presence of Mg^{2+} regardless of NaCl concentration in the range of 0–100 mM (Figure 3a,b). Divalent ions have much more pronounced effect on the adsorption behavior of negatively charged surfaces because they produce a shorter Debye length than monovalent electrolytes (at the same concentration).²⁰ In some cases poly(A) molecules tend to orient parallel (Figure 2b), but this effect is not so pronounced as in the previous case. At 1 mM of Mg^{2+} and 500 mM of NaCl the surface density of poly(A) molecules greatly increases (Figure 3c). Small nonfibrillar features in Figure 3a,b correspond to short fragments of poly(A) molecules, and large ones in Figure 3c, to poly(A) aggregates, which are formed in solution with high salt concentration.

In the case when the subphase contained 1 M NaCl and chelating agent (EDTA sodium salt, 10 mM), polynucleotides were not found on the substrate (Figure 4). Comparing this result with the results presented in Figure 2, we conclude that adsorption of poly(A) is mediated by divalent cations which are present in our used NaCl solution in a small amount (less

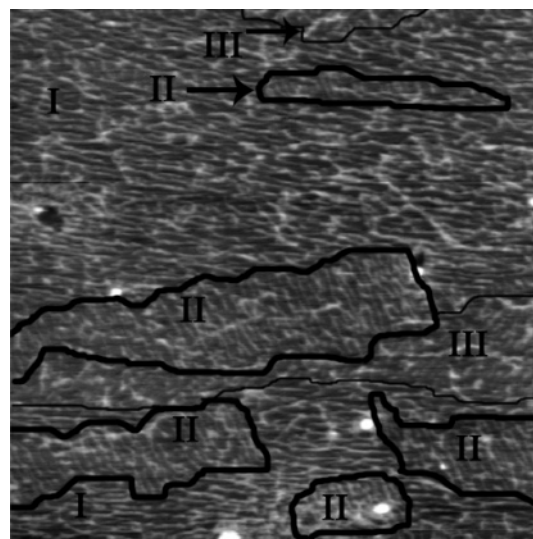


Figure 5. Analysis of poly(A) domains orientation on the example of the AFM image of stearic acid LB monolayers transferred from the subphase containing poly(A) (10^{-3} mg/mL) and 500 mM NaCl. Three types of domains are outlined and marked as I, II, and III.

than 0.01% by mass, see Materials and Methods, or in molar concentration less than 0.6 mM for MgCl_2).

We should emphasize that the results presented in the Figures 1–4 were highly reproducible including the dependence of coverage density on the monovalent salt concentration and self-organization effect presented in Figure 2.

The dependence of the adsorption density on the electrolyte concentration is well-known and can be explained as follows: by increasing the monovalent (or divalent) ion concentration the double-layer electrostatic repulsion of the two surfaces may be reduced as much as to let these surfaces approach each other and fall into the van der Waals attraction domain.²⁰ The small amount of divalent ions might be required to stabilize the structure, and to see the molecules by AFM because they are imaged in air, they could leave the surface during monolayer transfer unless some electrostatic (attractive) components are brought into play by the Mg ion impurities.

The orientation might be due to some epitaxial effect made possible by the quasi-equilibrium conditions ensured by the very low divalent ion concentration. We should emphasize the role of stearic acid monolayer in this orientation effect: we did not find the reports about similar structures on the mica surface with the same other “players” (nucleic acids and mono- and divalent ions), though such systems have been thoroughly studied.^{21,22} The role of the monolayer might be the following: the surface of the monolayer consists of the rows of hydrocarbon tails alternated with the rows of grooves which form well-ordered 2D structure. Similar structures were repeatedly ob-

served on different LB monolayers with AFM²³ and can be considered as 2D crystals. If divalent concentration is very small (and therefore the molecules have enough freedom), poly(A) molecules arrange along the grooves because here they have minimal potential energy. Arrangement of DNA molecules along the crystallographic axes was also observed on the graphite surface.²⁴ Analysis of poly(A) domains orientation shows that there are three types of domains outlined and numbered as I, II, and III in Figure 5, which is the same AFM image as in Figure 2d. The angles between the directions of polynucleotide molecules inside these domains constitute 60°. This angle indicates that the LB monolayer is probably packed into hexagonal structure on the mica surface.

Kinetic trapping conditions due to increased divalent ion concentration prevent this orientation effect from taking place. Divalent ions act as bridges between two negatively charged surfaces and therefore stabilize the negative charged molecular structure.²⁰

Conclusion

We have demonstrated here a new method of creation of self-organized nanostructures of long poly(A) molecules using simple Langmuir–Blodgett technique and transfer of the monolayer with polynucleotides onto a solid substrate. In the presence of a small amount of divalent cations and 0.5–1 M of sodium chloride in the subphase poly(A) molecules adsorb onto the surface of the stearic acid monolayer in domains which consist of stretched parallel threads. The angles between the directions of polynucleotides inside these domains constitute 60°. Monovalent ions make the adsorption possible due to Debye screening. Thus, the surface density of polynucleotide molecules in these domains can be governed by the monovalent ion concentration. Divalent ions stabilize the negative charged molecular structure: when divalent ion concentration is very low, this stabilization effect is weak, and therefore poly(A) molecules have enough freedom to adsorb along the grooves of a stearic acid monolayer; the increase of divalent ion concentration leads to kinetic trapping and therefore to the loss of the orientation effect.

Molecular self-assembly presents a “bottom-up” approach to the creation of objects specified with high precision. At the present time many systems with self-assembly of DNA have been developed which are based on complementary binding of DNA molecules.^{25,26} Fabrication of these systems requires computational design of the sequence of each molecule included in the structure and their further synthesis. In our work we report about another kind of self-assembly which is not based on specific interactions of complementary base pairs but is ruled just by electrostatic and van der Waals interactions at the surface of a stearic acid Langmuir–Blodgett monolayer.

Acknowledgment. This work is supported by INTAS Project No. 06-14-6323.

References and Notes

- (1) Zhou, X.; Wu, L.; Zhou, J. *Langmuir* **2004**, *20*, 8877–8885.
- (2) Lai, R. Y.; Seferos, D. S.; Heeger, A. J.; Bazan, G. C.; Plaxco, K. W. *Langmuir* **2006**, *22*, 10796–10800.
- (3) Boon, E. M.; Ceres, D. M.; Drummond, T. G.; Hill, M. G.; Barton, J. K. *Nat. Biotechnol.* **2000**, *18*, 1096–1100.
- (4) Stoltenberg, R. M.; Woolley, A. T. *Biomed. Microdevices* **2004**, *6*, 105–111.
- (5) Felgner, P. L.; Gadek, T. R.; Holm, M.; Roman, R.; Chan, H. W.; Wenz, M.; Northrop, J. P.; Ringold, G. M.; Danielsen, M. *Proc. Natl. Acad. Sci. U.S.A.* **1987**, *84*, 7413–7417.
- (6) Schouten, S.; Stroeve, P.; Longo, M. L. *Langmuir* **1999**, *15*, 8133–8139.
- (7) Antipina, M. N.; Gainutdinov, R. V.; Rachnyanskaya, A. A.; Tolstikhina, A. L.; Yurova, T. V.; Khomutov, G. B. *Surf. Sci.* **2003**, *532–535*, 1025–1033.
- (8) Kawaura, C.; Noguchi, A.; Furuno, T.; Nakanishi, M. *FEBS Lett.* **1998**, *421*, 69–72.
- (9) Sukhorukov, G. B.; Mohwald, H.; Decher, G.; Lvov, Y. M. *Thin Solid Films* **1996**, *284–285*, 220–223.
- (10) Markarian, M. Z.; Moussallem, M. D.; Jomaa, H. W.; Schlenoff, J. B. *Biomacromolecules* **2007**, *8*, 59–64.
- (11) Budker, V. G.; Kazatchkov, Yu. A.; Naumova, L. P. *FEBS Lett.* **1978**, *95*, 143–145.
- (12) Budker, V. G.; Godovikov, A. A.; Naumova, L. P.; Slepneva, I. A. *Nucleic Acids Res.* **1980**, *8*, 2499–2515.
- (13) McManus, J. J.; Ralder, J. O.; Dawson, K. A. *J. Phys. Chem. B* **2003**, *107*, 9869–9875.
- (14) Patil, S. D.; Rhodes, D. G.; Burgess, D. J. *AAPS J.* **2004**, *6*, 1–10.
- (15) Bhaumik, A.; Ramakanth, M.; Brar, L. K.; Raychaudhuri, A. K.; Rondelez, F.; Chatterji, D. *Langmuir* **2004**, *20*, 5891–5896.
- (16) Filonov, A. S.; Gavrilko, D. Yu.; Yaminsky, I. V. *FemtoScan SPM Image Processing Software Manual*; Advanced Technologies Center: Moscow, 2001; <http://www.nanoscopy.net/manual/en/>.
- (17) Lyubchenko, Y. L.; Gall, A. A.; Shlyakhtenko, L. S.; Harrington, R. E.; Jacobs, B. L.; Oden, P. I.; Lindsay, S. M.; *J. Biomol. Struct. Dyn.* **1992**, *10*, 589–606.
- (18) Smith, B. L.; Gallie, D. R.; Le, H.; Hansma, P. K. *J. Struct. Biol.* **1997**, *119*, 109–117.
- (19) Shao, Z.; Mou, J.; Czajkowsky, D. M.; Yang, J.; Yuan, J.-Y. *Adv. Phys.* **1996**, *45*, 1–86.
- (20) Muller, D. J.; Amrein, M.; Engel, A. *J. Struct. Biol.* **1997**, *119*, 172–188.
- (21) Hansma, H. G.; Laney, D. E. *Biophys. J.* **1996**, *70*, 1933–1939.
- (22) Rivetti, C.; Guthold, M.; Bustamante, C. *J. Mol. Biol.* **1996**, *264*, 919–932.
- (23) Reitzel, N.; Hassenkam, T.; Balashev, K.; Jensen, T. R.; Howes, P. B.; Kjaer, L. K.; Fechtenkötter, A.; Tchegobtareva, N.; Ito, S.; Mullen, L. K.; Bjornholm, T. *Chemistry* **2001**, *7*, 4894–4901.
- (24) Yamamoto, I.; Tanaka, H.; Kawai, T. *Jpn. J. Appl. Phys.* **2003**, *42*, 1559–1560.
- (25) Winfree, E.; Liu, F.; Wenzler, L. A.; Seeman, N. *Nature* **1998**, *394*, 539–544.
- (26) Rothmund, P. W. K. *Nature* **2006**, *440*, 297–302.

BM0702096